Original Article

Recurrent Regional Allelic Imbalance in Chromosome 15 in Rat Endometrial Adenocarcinomas

Ahmad Hamta, Ph.D.[1]*, Farah Talebbeigy, M.Sc.[2]

1. Biology Department, Faculty of Science, Arak University, Arak, Iran
2. Department of Molecular Biotechnology Biochemistry, University of Sydney, Sydney, Australia

**** Corresponding Address: P.O.Box: 879-38156, Biology Department, Faculty of Science, Arak University Arak, Iran***
Email: a-hamta@araku.ac.ir

Received: 15/Dec/2008, Accepted: 16/Aug/2009

Abstract

Objective: Animals of the inbred BDII rat strain are genetically predisposed to endometrial adenocarcinomas (EAC) and can be used to model human cancer. From our previous studies, it was obvious that some chromosomes were selectively involved in EAC development; one of them was rat chromosome (RNO) 15, in which there were often losses in the short arm and gains in the long arm. Since cytogenetic events lead to allelic imbalance and/or loss of heterozygosity (AI/LoH) in RNO15, it was subjected to a detailed analysis with polymorphic microsatellite markers spanning the entire chromosome.

Materials and Methods: BDII/Han females were crossed to males from two other inbred rat strains known to have low incidence of EAC (BN/Han and SPRD-*Cu3*/Han). DNA extracted from F1, F2 and backcross offspring were used in this studies. Our final marker panel consisted of 36 markers.

Results: The analysis showed that AI/LoH was common in EAC tumors and was concentrated to four well-defined regions along the chromosome. Two of these regions were close to the distal end of the short arm; one region was in the middle of the chromosome, probably spanning the centromere; and the fourth region was located distally in the long arm.

Conclusion: According to the Rat Genome Project (RGP), the number of genes in these regions approached 300. According to a database search, about 80 of these genes could be considered "cancer-related" and they were potential candidates to be targets for the observed chromosomal aberrations. Among the cancer-related genes, there were *Anxa7* (Region I), *Bmp4*, *Lgals3*, *Cdkn3* (Region II), *Rb1*, *Ddx26*, *Clu*, *Bnip3*, *Nkx3.1* (Region III), and *Gpc5* (Region IV).

Keywords: Rats Inbred Strains, Endometrial Cancer, LOH

Yakhteh Medical Journal, Vol 12, No 1, Spring 2010, Pages: 59-72

Introduction

The BDII inbred rat is genetically predisposed to develop endometrial cancer (EC) and can be used to model human cancer. In some studies to clarify the genetic factors behind cancer susceptibility and tumor development in the rat models, crosses between BDII rats and rats belonging to inbred strains resistant to EC, including subsequent intercrosses and backcrosses, has been performed and DNA from those animals and tumors are subjected to molecular genetic analysis (1-6).

We have shown that there is a pattern of recurrent chromosomal changes in developing tumors mainly involving six specific chromosomes (7). One of these chomosomes was chromosome rat (RNO15), in which losses were recorded in the short arm and/or gains in the long arm. In order to characterize these tumor-specific genetic aberrations in greater detail, we have submitted a series of endometrial adenocarcinoma (EAC) tumors to allelotyping with polymorphic microsatellite markers covering the entire length of RNO15.

Materials and Methods

Animal crosses, tumour samples and DNA extraction for CGH

The BDII inbred rat strain is known to exhibit a heritable susceptibility to EAC (8, 9). BDII/Han females were crossed to males from two other inbred rat strains known to have low incidence of EAC (BN/Han and SPRD-*Cu3*/Han). In order to generate F2 rats, the F1 animals were intercrossed. In addition, backcross populations were generated by crossing male F1 rats to female BDII rats. BDII strain development and all the crosses are under permission of Research Ethics Committee in Central Institute for Laboratory Animals, Department of Pathology, Hannover, Germany. The animals were palpated regularly for signs of tumor formation. Total tumor materials from both crosses were shown in table 1.

Table 1: Total tumor material from both crosses

	BN Cross				SPRD Cross				
	F1	F2	BC	Total	F1	F2	BC	Total	Grand Total
Total animal	18	59	105	182	17	54	103	174	356
Animals without tumor	6	36	65	107	10	23	59	92	199
Animals with benign tumor	1	5	9	15	5	20	7	32	47
Animals with malignant tumor	11	18	31	60	2	11	37	50	110
Out of them EAC	10	11	26	47	2	9	28	43	90
Out of them early EAC	5	9	12	26	1	6	13	23	49

When the presence of a tumor was in the size of a pea, the animal was sacrificed, then a piece of the tumor was subjected to cell culture and the other segment was used for DNA extraction from solid tumor. For the present study, materials of 45 tumors were analyzed, all of which had been pathologically characterized as endometrial adenocarcinomas (EAC; Table 2). (DNAs from both solid tumor materials (ST) and tissue cultures (TC) were available from 30 of the tumors, whereas only ST material was available from 11 tumors and TC material from four tumors.

Source of polymorphic markers

Primer pair sequences for microsatellite markers were obtained from available databases and synthesized by Sigma-Genosys, Cambridge, UK. We attempted to collect markers covering the entire genome with a maximum distance between adjacent markers of less than 5 cm. The markers were tested for polymorphism among the three inbred rat strains (BDII, BN and SPRD). Polymerase chain reaction (PCR) was carried out in 15 µl of a solution containing 100 ng of template DNA, 0.2 mM dNTP, 1.5 mM MgCl, and 0.2 mM from each primer containing 0.75 U Taq DNA polymerase (Advanced Biotechnologies, Epsom, UK) and ×1 PCR buffer (Advanced Biotechnologies). To prevent evaporation, the reaction mixtures were overlaid with 30 µl mineral oil. The amplification was performed in 96-well microtiter plates on an Omni Gene thermal cycler (Hybaid Ltd., Middlesex, UK), starting with 3mins denaturation step at 94°C, followed by 30 cycles of denaturing at 94°C for 30secs, annealing at 55°C for 30secs, extension at 72°C for 1min, and ending with a elongation step for 7mins at 72°C. The PCR products were separated on 4% Metaphor® agarose gel (BMA products, Rocklands, ME) in 1x TAE buffer by electrophoresis at 90V for 1-2hrs. Ethidium bromide staining was performed to make the DNA visible under UV light. The linkage map position of each informative marker was obtained from the integrated linkage maps in the RATMAP database, and the physical position was obtained from the Rat Genome Project build 2.1 (via the Ensembl or NCBI websites).

Allelic imbalance

For allelotyping, PCR was performed in 10 µl of the same solution under the same PCR conditions as the above, but with the forward primer labelled with a fluorochrome (6FAM, TET or HEX, primers purchased from Sigma-Genosys). Genomic DNA isolated from tumor cells (ST and/or TC) and normal liver material of the same animal was used as template. Based on differences in size and label, the PCR products in groups of 4-6 markers were pooled and the DNA was alcohol-precipitated. The pooled and dried sample mix was redissolved in 10 µl distilled water, then 2.0 µl of the sample was mixed with 2.1 µl formamide; 0.45 µl blue dextran ;and 0.45 µl Genescan-500TM ROX commercial size standard (PE Applied Biosystems, Foster City, CA), subsequently. The sample mix was denatured at 96°C for 3mins and kept on ice, until 1.5µl of sample was loaded in each lane on 5% denaturing polyacrylamide gels (Long Ranger gel, BMA products). The gels were preheated to 51°C, then run in ×1 tris borate EDTA (TBE) buffer on an automated ABI prism™, 377-96 collection Genescan instrument (PE Applied Biosystem), for 2.5hrs under the standard conditions recommended by the manufacturer. Microsatellite marker peak data were collected and analyzed with the Genescan and Genotyper analysis software. Presence of allelic imbalance was evaluated by calculating the allelic imbalance ratio", AIR=(T1/T2)/(N1/N2), where N1 and N2 are the peak heights for the curves representing alleles in normal tissue, and T1 and T2 are the corresponding peak heights for alleles in the tumor tissue from the same animal. If AIR value was above 1.0, inverted value was used in order to give AIR values between 0-1. PCR was carried out twice for each marker and each PCR product was separated twice on automated ABI prism™, 377-96 collection Genescan (PE Applied Biosystem), yielding four separate AIR values for each tumor.

Table 2: The tumour material: RUT tumors derived from F1 or F2 intercross animals, NUT tumors derived from backcross animals. "Age" refers to the age of the animal when it was sacrificed

Backcross	*Tumour designation*	*Solid tumour (ST)*	*Tumour culture (TC)*	*Age*	*Pathology*
BN strain	NUT9	+		543	EAC
	NUT31	+	+	640	EAC
	RUT7	+	+	662	EAC
	NUT46	+	+	666	EAC
	NUT43	+	+	670	EAC
	RUT 25		+	670	EAC
	NUT52	+	+	673	EAC
	RUT 12	+	+	677	EAC
	RUT 30	+	+	689	EAC
	NUT50	+	+	702	EAC
	NUT51	+	+	709	EAC
	NUT76	+	+	735	EAC
	NUT81	+	+	738	EAC
	NUT82	+	+	738	EAC
	NUT98	+	+	738	EAC
	NUT99	+	+	738	EAC
	NUT100	+	+	738	EAC
	NUT128	+	+	748	EAC
	NUT130	+	+	748	EAC
SPRD strain	NUT201	+		511	EAC
	RUT2	+	+	565	EAC
	RUT3		+	591	EAC
	RUT6		+	624	EAC
	NUT24		+	638	EAC
	NUT14	+		645	EAC
	NUT17	+	+	653	EAC
	NUT 203	+		654	EAC
	RUT 13	+	+	662	EAC
	NUT 20	+		666	EAC
	RUT 16		+	685	EAC
	NUT 12	+	+	688	EAC
	NUT 59	+		692	EAC
	NUT 35	+		704	EAC
	NUT 47	+	+	707	EAC
	NUT 49	+		711	EAC
	NUT 39	+	+	712	EAC
	NUT 33	+	+	714	EAC
	NUT 70	+		724	EAC
	NUT 72	+	+	728	EAC
	NUT 42	+	+	738	EAC
	NUT 202	+		741	EAC
	NUT 29	+		745	EAC
	NUT 55	+	+	747	EAC
	NUT 3	+	+	780	EAC

Results

Selection of microsatellite markers

Databases rat genome database (RGD) were consulted for polymorphic microsatellite markers on the entire length of RNO15. For unknown reasons, there seems to be relatively few markers on this chromosome compared to most other rat chromosomes (10), but we managed to collect 78 markers mapping to RNO15. Each marker was tested for performance under our PCR conditions. We were unable to establish a large enough set of markers that were informative in both crosses; we had to complement these ideal markers with subsets that were informative in only one of the crosses. Thus, our final set consisted of 36 markers that were informative in one or both of our crosses (Table 3).

As shown, coverage was reasonable across the entire length of the chromosome with an average spacing between markers of 4.0 Mb in the SPRD and 4.5 Mb in the BN cross. Even so, there was a segment with poor coverage in the middle of the chromosome.

Allelotyping of 45 EAC tumors

Based on previous genome-wide scans, 45 EAC tumors from animals were known to exhibit heterozygosity in all or part of RNO15. Most of the tumors were from back-cross animals (NUT tumors, average BDII-derived genetic content is 75% in these animals), but a few tumors came from F1 or F2 animals (RUT tumors, average BDII-derived genetic content is 50%). For most of the tumors, DNAs were available from both solid tumor material (ST) and tumor cell cultures (TC) except for a few only one or the other form of DNA, was available as shown in table 3. The average informative segment in each tumor was about 72 Mb among the ST and about 68 Mb in the TC. The total amount of informative RNO15 segment analyzed was about 2946 Mb of DNA in 41 ST and about 2377 Mb in 35 TC. The chromosomal distribution of each informative segment is shown in Figure 1 together with the results of the allelotyping. AIR values were calculated for each marker as described and AIR<0.60 was considered to be indicative of allelic imbalance (AI) at the marker locus (Fig 1), whereas a double letter signified AIR<015.

The latter limit was arbitrarily selected to indicate complete LOH at the marker locus. We compiled the data based on two different approaches. In table 3, the frequency of tumors exhibiting AI is shown for each marker locus, whereas the curves in figure 2 represent the average AIR value at each marker point. Both ways of treating the data give results that point in the same direction: there is a distinct tendency to non-random AI/LOH and the data set clearly demonstrates that there are 4 regions of recurrent AI along RNO15. It should be remembered that a reduced AIR value may be caused either by reduction or loss of one allele, or by gain or amplification of the other. In the case of RNO15, we know from Comparative genomic hybridization (CGH) analysis that there is often losses in the short arm (RNO15p), whereas gains are common in the long arm (RNO15q) 10. However, the actual situation in any particular case must be evaluated individually by combining cytogenetic and other information.

Delineation of AI/LOH regions

Thus, 4 regions of recurrent AI in EAC tumors are present in RNO15. The regions are positioned along the entire length of the chromosome. Based on the data in table 4 and figure 2, it is possible to make rough estimations of the position and size of these regions.

Thus, the first region encompasses four of the polymorphic markers which is used and situated distally in the short chromosome arm. The approximate position of this region can be estimated to be at the distal tip of RNO15p from position 0 Mb to about 10 Mb. The second region seems to be quite narrow and only includes a single one of the used markers (D15Rat5). This marker is located at 22.5 Mb and the region of recurrent AI may comprise a small band in the middle of RNO15p, maybe extending from 21 to 24Mb. The third region is located quite close to the centromere and may in fact extends from the proximal part of the short arm into the proximal portion of the long arm. Unfortunately, the exact position of the centromere has not yet been determined; furthermore, the coverage of polymorphic markers is poor in the proximal part of the long arm. Consequently, the extension and characteristics of this region cannot be determined with any great exactitude. Possibly, the region extends from about position 40 Mb to about 60 Mb. What should be noted is that, particularly in the BN cross, some segments of the region may be involved more often than others (see markers D15Wox9, D15Wox8, D15Rat72, D15Rat14 in Table 3). The fourth region again seems to be quite narrow involving markers close to the position 100 Mb, but maybe extend from about 98 Mb to about 104 Mb.

Table 3: Microsatellite markers used for allelic imbalance analysis of RNO15 in EAC tumours

Marker	Position (cM)	Ensembl (Mb)	Informative BN cross	Informative SPRD cross	Informative Both crosses
1 D15Rat109	0	1.0		+	
D15Rat129	0	1.6		+	
2 D15Rat159	9	8.5	+	+	+
3 D15Rat159	12	-	+	+	+
4 D15Rat77	14	13.8	+	+	+
5 D15Rat110	21	14.1		+	
6 D15Rat 54	19	14.5	+		
7 D15Rat136	21	16.4	+		
8 D15Mit2	25	18.7	+		
9 D15Mgh7	26	22.5	+	+	
10 D15Rat5 26	21	24.6		+	+
11 D15Rat130	20	25.1		+	
12 D15Rat160	38	32.6	+		
13 D15Rat83	35	37.3		+	
14 D15Rat170	40	37.9	+	+	
15 D15Rat141	34	38.4	+	+	+
16 D15Got34	38	38.4	+	+	+
17 D15Arb1 38	45	43.8		+	+
18 D15Rat13	45	-	+	+	
19 D15Mit7 45	44	45.4	+	+	+
20 D15Wox9	44	45.4		+	+
21 D15Wox8	54	45.6	+	+	
22 D15Rat72	48	45.9	+	+	+
23 D15Rat14	60	72.3	+		+
24 D15Rat21	60	72.9		+	
25 D15Rat47	62	80.4	+	+	
26 D15Mgh8	67	83.4	+		+
27 D15Mgh4	68	84.1	+	+	
28 D15Rat40	71	84.9		+	+
29 D15Rat166	70	89.6	+		
30 D15Mgh9	73	91.6	+		
31 D15Got82	75	96.4		+	
32 D15Got84	79	100.0	+	+	
33 D15Rat26	81	100.7		+	+
34 D15Rat25	81	100.8			
35 D15Rat155	87	10.4	+	+	
36 D15Rat29	87	10.8	+		+
Total length RNO15	87	109.8			
No. of markers	36	36	24	27	15
Average distance (cM)	2.4	--	3.2	3.1	5.2
Average distance (Mb)	--	2.9	4.5	4.0	7.2

Table 4: Frequency of AI/LOH (AIR≤0.60) in EAC tumors at polymorphic markersa-long RNO15. Data clearly show four regions of elevated AI/LOH frequency (grey background color)

		Marker		Percent of tumours exhibiting allelic imbalance at marker				
		Position		SPRD cross		BN cross		
No.	Marker	cM	Mb	ST	TC	ST	TC	Average
1	D15Rat109	0	1.0	50	50	-	-	50
2	D15Rat129	0	1.6	50	60	-	-	55
3	D15Rat159	9	8.5	56	60	64	79	65
4	D15Rat77	12	-	56	50	64	86	64
6	D15Rat110	14	13.8	13	22	14	21	18
7	D15Rat54	21	14.1	13	22	-	-	18
8	D15Rat136	19	14.5	-	-	14	14	14
5	D15Mit2	21	16.4	-	-	21	21	21
9	D15Mgh7	25	18.7	-	-	13	20	17
10	D15Rat5	26	22.5	68	62	62	85	69
11	D15Rat130	21	24.6	22	23	-	-	23
12	D15Rat160	20	25.1	22	15	-	-	19
13	D15Rat83	38	32.6	-	-	15	23	19
14	D15Rat170	35	37.3	56	64	-	-	60
15	D15Rat141	40	37.9	33	43	46	58	45
16	D15AGot34	34	38.4	50	36	46	58	48
17	D15RArb1	38	38.4	67	64	46	58	59
18	D15Rat13	45	43.8	50	43	-	-	46
19	D15Mit7	45	-	50	43	54	75	55
20	D15Wox9	44	45.4	59	62	85	92	74
21	D15Wox8	44	45.4	53	62	-	-	57
22	D15Rat72	54	45.6	71	62	85	92	77
23	D15Rat14	48	45.9	71	54	77	92	73
24	D15Rat21	60	72.3	-	-	8	25	17
25	D15Rat47	60	73.0	14	11	-	-	13
26	D15Mgh8	62	80.4	15	13	15	23	17
27	D15Mgh4	67	83.4	-	-	14	21	18
28	D15Rat40	68	84.1	8	13	14	21	14
29	D15Rat166	71	84.9	8	13	-	-	10
30	D15Mgh9	70	89.6	-	-	15	23	19
31	D15Got82	73	91.6	-	-	8	23	15
32	D15Got84	75	96.4	15	0	-	-	8
33	D15Rat26	79	100.0	54	100	69	69	73
34	D15Rat25	81	100.7	54	100	-	-	77
35	D15Rat155	81	100.8	-	-	77	69	73
36	D15Rat29	87	108.4	8	50	0	38	24

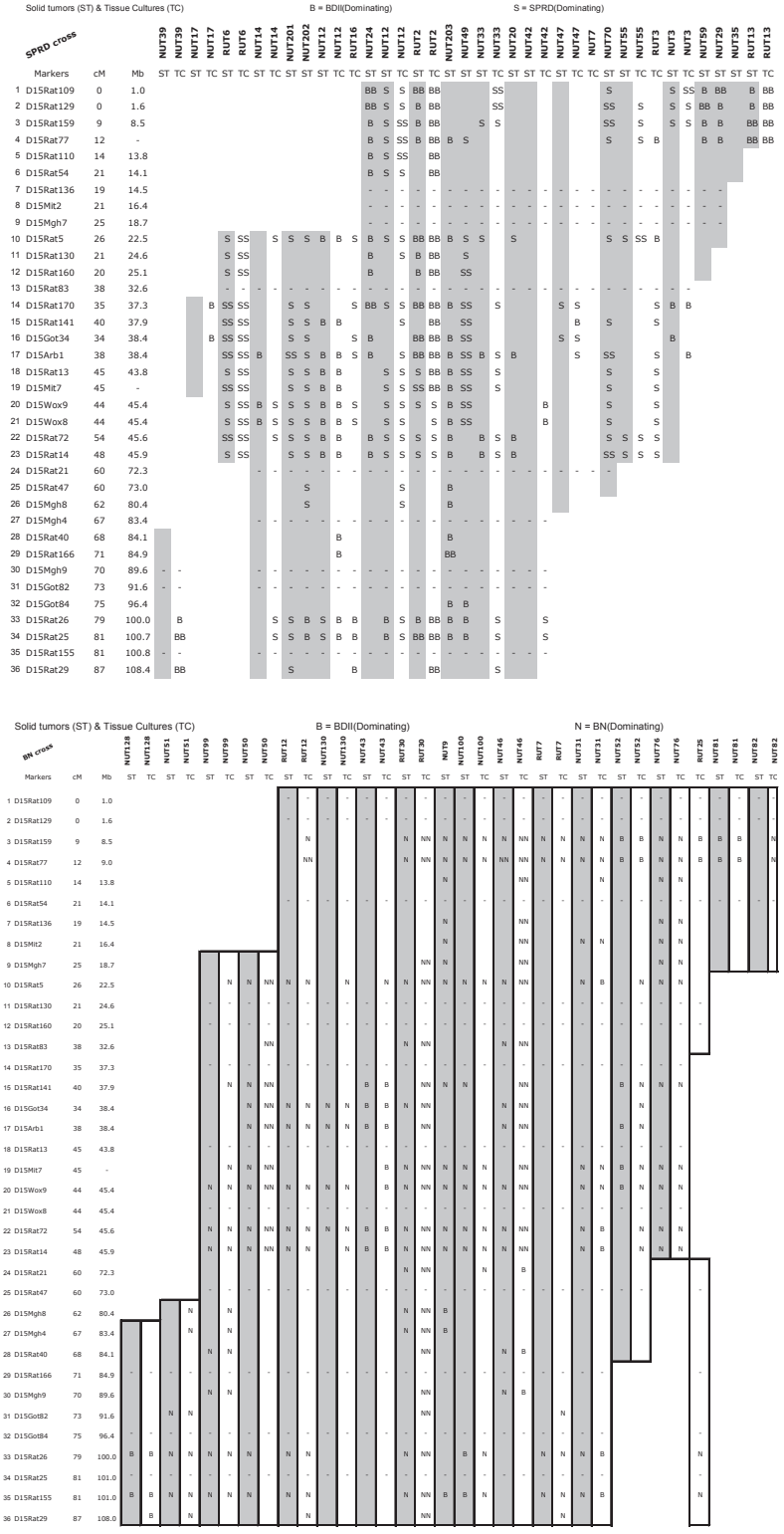

Fig 1: Diagrammatical representations of findings of AI/LoH in 45 EAC tumors from crosses involving susceptible BDII rats and non-susceptible (A) SPRD and (B) BN rats. Designations for the RNO15 microsatellite markers used are shown on the left, along with marker positions in cM (centimorgan) and Mb. Bars represent the extent of informative (heterozygous) RNO15 regions (grey bars = ST; white bars = TC) and letters inside bars indicated degree of AI. Two letters indicate AIR<0.15, one letter 0.15≤AIR≤0.60, no marking AIR>0.60, dash (-) uninformative or no data (B or BB = BDII allele dominating, N or NN = BN allele dominating, S or SS = SPRD allele dominating).

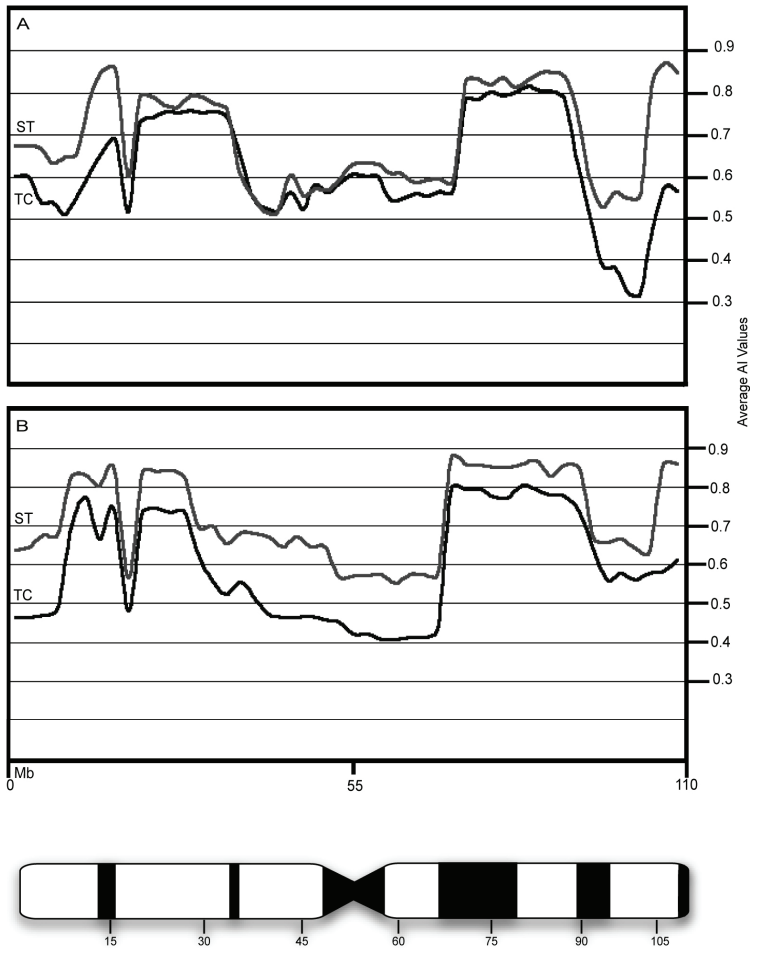

Fig 2: Curves representing the average AIR value at each marker along the length of RNO15. Grey curves: average AIR values from solid tumor (ST) DNA, Black curves: average AIR values from tumor tissue culture (TC) DNA. EAC tumors from (A) SPRD and (B) BN crosses. Approximate physical positions of markers can be estimated on the RNO15 ideogram at the bottom.

Table 5: The number of genes in the four regions of recurrent AI on RNO15

Region	Approx borders	Total genes [1)]	Known genes [2)]	Cancer-related genes [3)]
I	0-10 Mb	89	35	12
II	21-24 Mb	37	18	9
III	40-55 Mb	139	86	54
IV	98-104 Mb	22	10	5

[1)] ***Data taken from the Rat Genome Project build 2.1***
[2)] ***Data collected using comparative mapping between rat, mouse and human as described***
[3)] ***Data collected from the following databases:***
http://caroll.vjf.cnrs.fr/cancergene/Aonco_consult.html
http://www.infobiogen.fr/services/chromcancer/Indexbyalpha/idxa_A.html

Genes in the regions of recurrent AI

The approximate number of genes in each region can be obtained from the Ensembl or NCBI databases (Table 5).

Presently, the situation with respect to assigning function to the rat genes is unsatisfactory. For most genes that are defined their specific positions in the rat draft sequence, there is only one locus designation but no defined biochemical or functional assignment. Recently, in the Ensembl database, putative genes have been subjected to cross-species comparison with respect to sequence similar-

ity and those generating a "unique best reciprocal hit (UBRH)" 3 which have been predicted to be the true ortholog. For putative genes in the regions of recurrent AI, we have determined whether UBRH hypothesis is possible, in addition, we have checked whether the position of the predicted ortholog is situated inside segments of conserved orthology in rat, mouse and human (Fig 3).

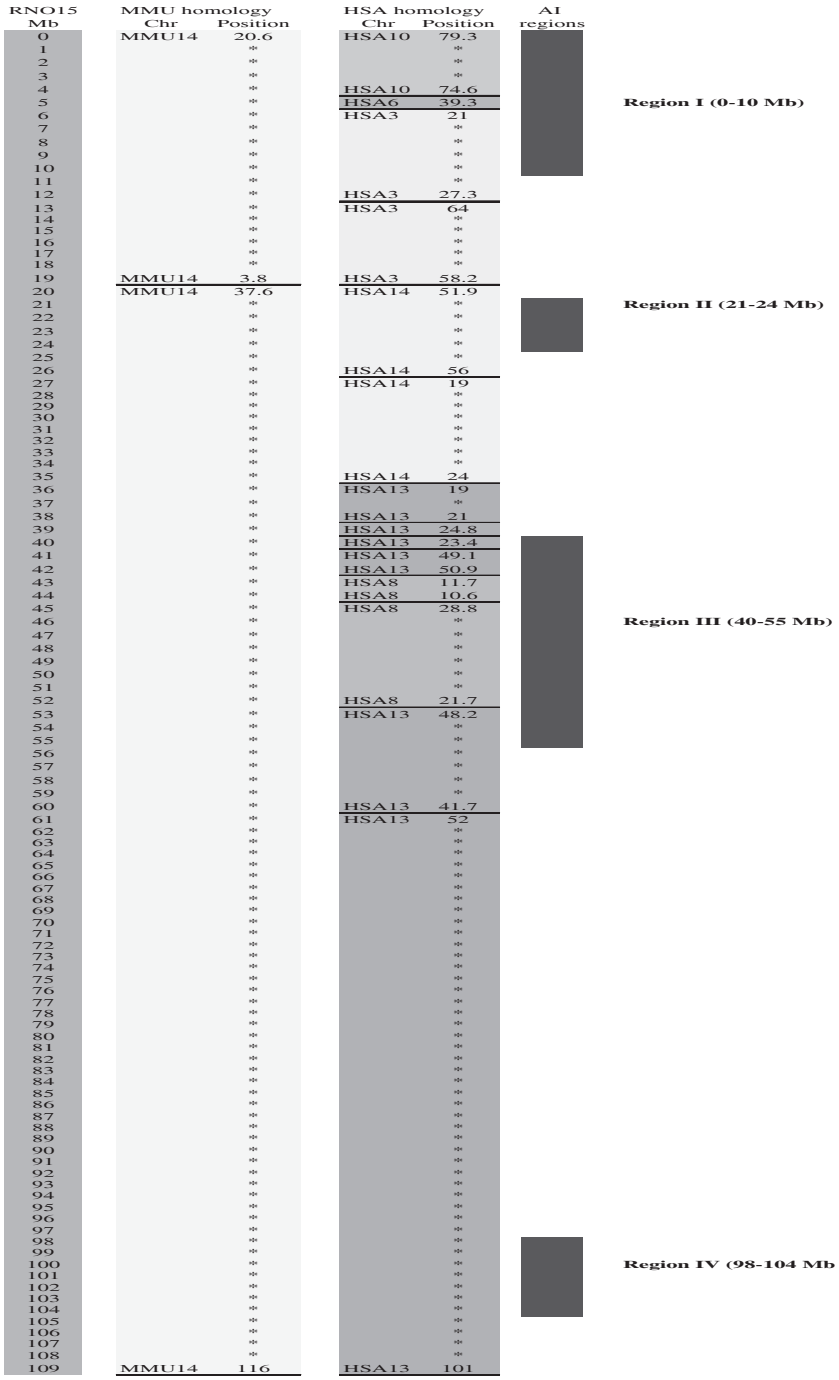

Fig 3: RNO15 comparative mapping. On the left the Mb positions along the 109 mB of RNO15 are indicated, and the homologous segments in the mouse (center) and human (right) are shown. Note that, in essence, the entire gene content of RNO15 seems to be conserved in two mouse chromosomal segments (both located on MMU14), whereas there are (at least) 14 separate homologos segments in humans (two in HSA3, one on HSA6, two on HSA8, one on HSA10, six on HSA13, two on HSA14). The homology data were taken into account for the identification and annotation of the genes on RNO15 as described in the text. On the far right, the positions of the regions of recurrent AI in rat EACs have been indicated (red bars).

If both criteria were fulfilled, we have assumed that the gene locus represents the true ortholog and changed the locus designation, accordingly. As a consequence of this analysis, a sizable subset of the putative genes in the regions of recurrent AI could be elevated to a known gene status (Table 5). We have checked these known genes against several databases containing cancer-related genes, as shown in table 5; a subset of the known genes are found to be listed as cancer-related genes and could be considered as the targets in the recurrent AI regions. These genes have been written in bold type in the Appendix. In addition, any gene with unknown function situated within the regions must be considered as potential candidates.

Discussion

The CGH findings in rat EAC tumors distinctly showed that RNO15 was often involved in chromosomal aberrations. It appeared that deletions were common in the short arm whereas addition were common in the long arm (2, 7). CGH is a method with many advantages; the most important of them is that entire spectrum of chromosome aberrations leading to copy number change in a tumor can be evaluated in a single experiment. However, the method also has some limitations, particularly with respect to sensitivity and resolution (11). Thus, only copy number changes at a gross chromosomal level can be detected by CGH analysis. Allelotyping analysis has potential to detect changes in small chromosome regions, consequently this method can be useful for verifying aberrations indicated from the CGH analysis and elucidating their molecular details. Furthermore, allelotyping analysis can be much more sensitive than CGH in detecting subtle changes on the molecular level, since resolution can be further improved by adding new polymorphic markers in the region by adding new polymorphic markers in the region. A drawback with alleltyping analysis is restricted to chromosome segments that are informative (heterozygous).

In the present study, a set of 36 microsatellite markers covering the entire length of RNO15 were used to assess AI along the chromosome. Existing AI was evaluated using two different approaches: For each marker (12) the frequency of tumors exhibiting AIR values of less than 0.6 was determined, and (1) the average AIR value across all tumors was calculated (Table 4 and Fig 2). Obviously, the two calculations are not independent, but they both pointed in the same direction: there are four well separated chromosome regions in RNO15 affected by AI interspaced sizable segments with little or no AI. Furthermore, the analysis clearly showed that the patterns were very similar when DNA from ST and TC were compared or when DNA from tumor sets derived from the two different crosses was compared. Two of the regions appeared to be quite narrow (regions II and IV), whereas region I and (in particular) region III were less distinctly defined. Adding to the difficulties in fully characterizing region III was (a) that it contains the centromeric heterochromatic segment and (b) that we were unable to find informative markers defining one of the borders of the region (see Table 3; gap between markers No. 23 and 24).

A greatly reduced AIR value is usually interpreted as complete LOH (AIR values below 0.15 are shown as a double letter Fig 2) and would then mean that one allele is completely absent due to loss, deletion, or somatic crossing-over. However, a very low AIR value could also be obtained if an allele is highly amplified and completely overshadows the other allele. More moderately, reduced AIR values are even more difficult to interpret. One possibility is that a subpopulation of the tumor cells exhibit complete LOH and that other cells (infiltrating normal cells or a deviating subpopulation of tumor cells) have no AI. Another possibility is that there is not complete LOH. For instance, if a chromosome segment is duplicated leading to trisomy, the theoretical AIR value is 0.66, quite close to our cut-off limit of AIR<0.6. In any case, whenever one allele is dominance; it should be kept in mind that this could be caused by either an increase of this allele or a true reduction of the other allele or a combination of both. This is of practical importance for the interpretation, since if there is loss/reduction of an allele; one might speculate that it is linked to a growth-inhibiting tumor suppressor gene, which is eliminated, whereas increase/gain of an allele may be an indication that the locus is linked to a growth-stimulating oncogene, which is amplified.

In an allelotyping study, it is determined from which one of the parental strains of the dominating allele is derived at a locus exhibiting AI. If the dominating allele is more often derived from one of the strains, this may be an indication of linkage to a strain-specific predisposing cancer-related gene.

In the backcross tumor material studied, we found a distinct difference between the two crosses in AI allele preferences (Fig 1).

Looking at the BN cross, it is clear that when AI occurs in RNO15; the BN-derived allele seems

to be preferentially retained in all four regions (BN allele dominating: Region I=78%, Region II=100%, Region III=82%, Region IV=74%). In contrast, in the SPRD cross, there was no clear cut strain preference of the allele retained. In fact, the values are close to 50% in all four regions (SPRD allele dominating: Region I=38%, Region II=64%, Region III=59%, Region IV=29%). These findings emphasize the importance of differences in the genetic make-up for the paths taken in tumor development. Studies have shown that there are significant differences in which susceptibility genes are active in these different crosses (4, 5). One finding which may be of particular significance is that dominating allele in different segments of the chromosome is derived from different parents that it is quite common among these tumors (see Fig 1). This is probably a reflection of the fact that RNO15 appears to be particularly prone to breakage and unbalanced translocations/ deletions as detected by cytogenetic studies (13). The involvement of RNO15 in chromosome aberrations during EAC development appears to be very dynamic.

At the present stage, one can speculate about the reason for the selective involvement of the four RNO15 regions. As shown in Table 4, quite a few genes known to be cancer-related are located in these regions (particularly true for the large Region III). Furthermore, it is quite possible that the target genes are to be found among the genes to which no function has yet been assigned. It is known that RNO15 is homologous to segments of human chromosomes (HSA) 10q, 6p, 3p, 14q, 8p, and 13q (Fig 3). Most of these chromosome segments are known to exhibit LOH in human endometrial cancer (2, 14-18) and in other human cancers (18, 19). Example of a cancer-related gene situated in Region I is *Anxa7*, whose human counterpart *ANXA7* (annexin A7) is located in 10q21, a chromosome band thought to harbor a suppressor gene associated with prostate cancer as well as other tumor types (20). This is not far from the position where a tumor suppressor gene in endometrial cancer has been localized (not yet characterized at HSA10q25; (16). Among cancer-associated genes in Region II is Bmp4 (bone morphogenic protein 4). The human homolog of this gene is known to be involved in poorly differentiated gastric cancer cell lines (21) as well as in bone and soft-tissue sarcomas (22), and has an important role in differentiation and tumor suppression in human cancer cells (23, 24). Lgals3 (lectin, galactoside-binding, soluble, 3), whose human homolog is known to be involved in endometrial cancer (25), breast cancer (26), colorectal cancer progression and metastasis (27), is another cancer-associated gene. Another important gene in Region II is *Cdkn3* (cyclin-dependent kinase inhibitor 3) which is involved in multiple-step hepatocarcinogenesis (28), human breast and prostate cancer (29).

The main part of Region III corresponds to HSA8p21 and part of HSA13q14.2. The latter chromosome segment contains the important RB1 tumor suppressor gene that is involved in cell cycle regulation (30). RB1 has been shown to play an important role in endometrial carcinogenesis in humans (31). However, LOH, which is located separately but adjacent to RB1 without reduction of RB1 expression, has been also been appeared in various sporadic cancers including: carcinomas of the head and neck, breast, ovary, prostate and other sites, suggesting the presence of a tumor suppressor gene. Thus, (32) identified a candidate tumor suppressor gene which they designated DICE1 (for deletion in cancer 1, the official symbol is *DDX26* for DEAD/H, Asp-Glu-Ala-Asp/His, box polypeptide 26) in the critical LOH region at HSA13q14.12-q14.2. In Region III, there are many other cancer-related genes that may be targets, e g *Tnfrsf19* (tumor necrosis factor receptor superfamily, member 19), whose human homolog (at HSA13q12) is known to be involved in apoptosis control (33). In the segment of Region III corresponding to HSA8p21, there are also numerous cancer-related loci known to be frequently engaged in LOH. One is *Bnip3l* (BCL2/adenovirus E1B 19kDa interacting protein 3-like), whose gene product interacts with anti-apoptotic proteins (34-37) and another is Nkx3.1 (NK3 transcription factor related, locus 1, *Drosophila*) for which the human homolog shows involvement in prostate tumorigenesis (38-40). Another gene in the region is clusterin (*Clu*) that exhibits elevated expression in human and murine intestinal neoplasia (41). Thus, there are numerous candidates in the large Region III. In contrast, quite few candidate genes were found in the small Region IV. This segment corresponds to distal HSA13q, a region of particular interest, because frequent copy number gains are common in certain human malignancies (42, 43). Genomic alterations including amplifications have also been implicated in certain types of human cancers including lung cancers and squamous cell carcinoma of the head and neck (44, 45). It also attempted to characterize a common region of amplification in 13q21-22 by FISH in order to explore what genes might

be targets for the amplification events. Even though, the region they defined was relatively large, (about 4 Mb) they only found a single true gene in the region. However, this gene (*GPC5*, glypican 5) was over expressed in lymphoma lines with HSA13q amplification. Since we have found that copy number increases are common in the distal part of RNO15q, the rat *Gpc5* homolog may be considered a target candidate in Region IV of our EAC tumors. Another possible target could be the *Dct* (dopachrome tautomerase) gene, which is known to be involved in melanoma (46, 47) and in malignant gliomas (48).

Conclusion

CGH analysis showed that RNO15 is frequently affected by copy number changes in rat EAC tumors. Allelotype analysis provided the means to scrutinize the chromosome on the molecular level, and we could conclude that there are four distinct regions in RNO15 that exhibit elevated levels of AI. These findings suggest that several genes important in rat EAC development are located in these regions. Further research is needed to identify these genes, but the human homologs are likely to be important in human cancer, since the corresponding homologous chromosome regions have been shown to be involved in aberration in human EAC and/or in other types of human malignancies.

Acknowledgments

This study was supported by grants from the Swedish Cancer Society, the Erik Philip-So¨rensen Foundation, the Nilsson-Ehle Foundation, the IngaBritt and Arne Lundberg Research Foundation, and the Adlerbertska Foundation.
The authors have no conflict of interest.

References

1. Behboudi A, Levan G, Hedrich HJ,Klinga-Levan K.High-density marker loss of heterozygosity analysis of rat chromosome 10 in endometrial adenocarcinoma. Gene Chromosome Canc. 2001; 32: 330-341.
2. Helou K, Walentinsson A, Beckmann B, Johansson A, Hedrich HJ, Szpirer C, et al.Analysis of genetic changes in rat endometrial carcinomas by means of comparative genome hybridization. Cancer Genet Cytogen. 2001; 127: 118-127.
3. Karlsson A, Helou K, Walentinsson A, Hedrich HJ, Szpirer C, Levan G. Amplification of Mycn, Ddx1, Rrm2, and Odc1 in rat uterine endometrial carcinomas. Genes Chromosomes Cancer. 2001; 31: 345-356.
4. Roshani L, Mallon P, Sjostrand E, Wedekind D, Szpirer J, Szpirer C, et al.Genetic analysis of susceptibility to endometrial adenocarcinoma in the BDII rat model. Cancer Genet Cytogen. 2005; 158: 137-141.
5. Roshani L, Wedekind D, Szpirer J, Taib Z, Szpirer C, Beckman B, et al.Genetic identification of multiple susceptibility genes involved in the development of endometrial carcinoma in a rat modelr. Int J Cancer. 2001; 94: 795-799.
6. Walentinsson A, Helou K, Wallenius V, Hedrich HJ, Szpirer C,Levan G.Independent amplification of two gene clusters on chromosome 4 in rat endometrial cancer: identification and molecular characterization. Cancer Res. 2001; 61: 8263-8273.
7. Hamta A, Adamovic T, Helou K,Levan G.Cytogenetic aberrations patterns in spontaneous endometrial adenocarcinomas in a rat model as revealed by chromosome banding and comparative genome hybridization. Cancer Genet Cytogen. 2004; in press:
8. Deerberg F,Kaspareit J.Endometrial carcinoma in BDII/Han rats: model of a spontaneous hormone-dependent tumor. J Natl Cancer Inst. 1987; 78: 1245-1251.
9. Kaspareit-Rittinghausen J, Deerberg F,Rapp K.Mortality and incidence of spontaneous neoplasms in BDII/Han rats. Versuchstierked. 1987; 30: 209-216.
10. Bihoreau M-T, Gauguier D, Kato N, Hyne G, Lindpaintner K, Rapp JP, et al.A linkage map of the rat genome derived from three F2 crosses. Genome Res. 1997; 7: 434-440.
11. Piper J, Rutovitz D, Sudar D, Kallioniemi A, Kallioniemi OP, Waldman FM, et al.Computer image analysis of comparative genomic hybridization. Cytometry. 1995; 19: 10-26.
12. Ambros RA, Vigna PA, Figge J, Kallakury BV, Mastrangelo A, Eastman AY, et al.Observations on tumor and metastatic suppressor gene status in endometrial carcinoma with particular emphasis on p53. Cancer. 1994; 73: 1686-1692.
13. Hamta A, Adamovic T, Heloua K. Göran Levan Cytogenetic aberrations in spontaneous endometrial adenocarcinomas in the BDII rat model as revealed by chromosome banding and comparative genome hybridization. Cancer Genet Cytogenet. 2005; 159 (2): 123-128.
14. Niederacher D, An HX, Cho YJ, Hantschmann P, Bender HG,Beckmann MW.Mutations and amplification of oncogenes in endometrial cancer. Oncology. 1999; 56: 59-65.
15. Okamoto A, Sameshima Y, Yamada Y, Teshima S, Terashima Y, Terada M, et al.Allelic loss on chromosome 17p and p53 mutations in human endometrial carcinoma of the uterus. Cancer Res. 1991; 51: 5632-5635.
16. Peiffer-Schneider S, Noonan FC, Mutch DG, Simpkins SB, Herzog T, Rader J, et al.Mapping an endometrial cancer tumor suppressor gene at 10q25 and development of a bacterial clone contig for the consensus deletion interval. Genomics. 1998; 52: 9-16.
17. Simpkins SB, Peiffer-Schneider S, Mutch DG, Gersell D,Goodfellow PJ.PTEN mutations in endometrial cancers with 10qLOH: additional evi-

dence for the involvement of multiple tumor suppressors. Gynecol Oncol. 1998; 71: 391-395.
18. Tritz D, Pieretti M, Turner S,Powell D.Loss of heterozygosity in usual and special variant carcinomas of the endometrium. Hum Pathol. 1997; 28: 607-12.
19. Bièche I,Lidereau R.Loss of heterozygosity at 13q14 correlates with RB1 gene underexpression in human breast cancer. Mol Carcinogen. 2000; 29: 151-158.
20. Srivastava M, Bubendorf L, Srikantan V, Fossom L, Nolan L, Glasman M, et al.ANX7, a candidate tumor suppressor gene for prostate cancer. Pro Natl Sci USA. 2001; 98: 4575-4580.
21. Katoh M,Terada M.Overexpression of bone morphogenic protein (BMP)-4 mRNA in gastric cancer cell lines of poorly differentiated type. J Gastroenterol. 1996; 31: 137-9.
22. Yoshikawa H, Rettig W, Lane J, Takaoka K, Alderman E, Rup B, et al.Immunohistochemical detection of bone morphogenetic proteins in bone and soft-tissue sarcomas. Cancer. 1994; 74: 842-7.
23. Kim J, Crooks H, Dracheva T, Nishanian T, Singh B, Jen J, et al.Oncogenic beta-catenin is required for bone morphogenetic protein 4 expression in human cancer cells. Cancer Res. 2002; 62: 2744-8.
24. Nishanian T, Kim J, Foxworth A,Waldman T.Suppression of tumorigenesis and activation of Wnt signaling by bone morphogenetic protein 4 in human cancer cells. Cancer Biol Ther. 2004; 3: 676-678.
25. van den Brule F, Buicu C, Berchuck A, Bast RD, M., Liu F, Cooper D, et al.Expression of the 67-kD laminin receptor, galectin-1, and galectin-3 in advanced human uterine adenocarcinoma. Hum Pathol. 1996; 27: 1185-1191.
26. Ochieng J, Warfield P, Green-Jarvis B,Fentie I.Galectin-3 regulates the adhesive interaction between breast carcinoma cells and elastin. J Cell Biochem. 1999; 75: 505-14.
27. Nakamura M, Inufusa H, Adachi T, Aga M, Kurimoto M, Nakatani Y, et al.Involvement of galectin-3 expression in colorectal cancer progression and metastasis. Int J Oncol. 1999; 15: 143-148.
28. Yeh C, Lu S, Chen T, Peng C,Liaw Y.Aberrant transcripts of the cyclin-dependent kinase-associated protein phosphatase in hepatocellular carcinoma. Cancer Res. 2000; 60: 4697-700.
29. Lee S, Reimer C, Fang L, Iruela-Arispe M,Aaronson S.Overexpression of kinase-associated phosphatase (KAP) in breast and prostate cancer and inhibition of the transformed phenotype by antisense KAP expression. Mol Cell Biol. 2000; 20: 1723-1732.
30. Dryja TP, Mukai S, Petersen R, Rapaport JM, Walton D,Yandell DW.Parental origin of mutations of the retinoblastoma gene. Nature. 1989; 339: 556-558.
31. Hamta A, Adamovic T, Heloua K, Levan G. Cytogenetic aberrations in spontaneous endometrial adenocarcinomas in the BDII rat model as revealed by chromosome banding and comparative genome hybridization. Cancer Genet Cytogenet, 2005; 159(2): 123-128.
32. Wieland I, Arden KC, Michels D, Klein-Hitpass L, Bhm M, Viars CS, et al. Isolation of DICE1: a gene frequently affected by LOH and downregulated in lung carcinomasr. Oncogene. 1999; 18: 4530-4537.
33. Wu GS, Burns TF, McDonald 3rd ER, Jiang W, Meng R, Krantz ID, et al.KILLER/DR5 is a DNA damage-inducible p53-regulated death receptor gene. Nat Genet. 1997; 17: 141-143.
34. Chen G, Cizeau J, Vande Velde C, Park JH, Bozek G, Bolton J, et al.Nix and Nip3 form a subfamily of pro.apoptotic mitochondrial proteins. J Biol Chem. 1999; 274: 7-10.
35. Matsushima M, Fujiwara T, Takahashi E, Minaguchi T, Eguchi Y, Tsujimoto Y, et al.Isolation, mapping, and functional analysis of a novel human cDNA (BNIP3L) encoding a protein homologous to human NIP3. Gene Chromosomes Cancer. 1998; 21: 230-235.
36. Sowter HM, Ratcliffe PJ, Watson P, Greenberg AH,Harris AL.HIF-1-dependent regulation of hypoxic induction of cell death factors BNIP3 and NIX in human tumors. Cancer Res. 2001; 61: 6669-6673.
37. Sun JL, He XS, Yu YH,Chen ZC.Expression and structure of BNIP3L in lung cancer. Ai Zheng. 2004; 23: 8-14.
38. Bhatia-Gaur R, Donjacour AA, Sciavolino PJ, Kim M, Desai N, Young P, et al.Roles for Nkx3.1 in prostate development and cancer. Genes Dev. 1999; 13: 966-77.
39. He WW, Sciavolino PJ, Wing J, Augustus M, Hudson P, Meissner PS, et al.A novel human prostate-specific, androgen-regulated homeobox gene (NKX3.1) that maps to 8p21, a region frequently deleted in prostate cancer. Genomics. 1997; 43: 69-77.
40. Xu LL, Srikantan V, Sesterhenn A, Augustus M, Dean R, Moul JW, et al.Expression profile of an androgen regulated prostate specific homeobox gene NKX3.1 in primary prostate cancerr. J Urology. 2000; 163: 972-979.
41. Chen X, Halberg RB, Ehrhardt WM, Torrealba J,Dove WF.Clusterin as a biomarker in murine and human intestinal neoplasia. Pro Natl Acad Sci USA. 2003; 100: 9530-9535.
42. Mao X, Lillington D, Child F, Russell-Jones R, Young B,Whittaker S.Comparative genomic hybridization analysis of primary cutaneous B-cell lymphomas: identification of common genomic alterations in disease pathogenesis. Gene Chromosomes Cancer. 2002; 35: 144-155.
43. Neat MJ, Foot N, Jenner M, Goff L, Ashcroft K, Burford D, et al.Localisation of a novel region of recurrent amplification in follicular lymphoma to an approximately 6.8 Mb region of 13q32-33. Gene Chromosomes Cancer. 2001; 32: 236-243.
44. Knuutila S, Bjorkqvist AM, Autio K, Tarkkanen M, Wolf M, Monni O, et al.DNA copy number amplifications in human neoplasms: review of comparative genomic hybridization studies. AM J Pathol. 1998; 152: 1107-1123.
45. Yu W, Inoue J, Imoto I, Matsuo Y, Karpas A,Inazawa J.GPC5 is a possible target for the 13q31-q32 amplification detected in lymphoma cell

lines. J Hum Genet. 2003; 48: 331-335.
46. Kawakami Y, Dang N, Wang X, Tupesis J, Robbins PF, Wang RF, et al.Recognition of shared melanoma antigens in association with major HLA-A alleles by tumor infiltrating T lymphocytes from 123 patients with melanoma. J Immuno ther. 2000; 23: 17-27.
47. Rad HH, Yamashita T, Jin HY, Hirosaki K, Wakamatsu K, Ito S, et al.Tyrosinase-related proteins suppress tyrosinase-mediated cell death of melanocytes and melanoma cells. Exp Cell Res. 2004; 301: 338.
48. Prins RM, Odesa SK, Liau LM. Immunotherapeutic targeting of shared melanoma-associated antigens in a murine glioma model. Cancer Res. 2003; 63: 8487-8491.